

Advanced DataSens™ Fiber Cables Enabling Distributed Acoustic Sensing for Structural Health and Security Monitoring

B. Zhu^{*a}, P. Westbrook^a, C. Guo^a, R. Pynn^b, X. Sun^b, B. Blakely^b, K. Stone^c, R. Knight^c, B.

Rinehart^c, A. McCurdy^d, M. Boxer^d, N. Hagelund^c, A. Gough^f, P. Kightley^f, P. Hubbard^g

^aLightera Labs, Somerset, NJ, USA; ^bLightera, Avon CT, USA, ^cLightera, Carrollton, GA, USA, ^dLightera, Norcross, GA, USA, ^eLightera, Denmark, ^fSintela, Bristol UK, ^gFiberSense, California USA

*Benyuan.zhu@lightera.com

ABSTRACT

Fiber optic distributed acoustic sensing (DAS) has recently gained significant attention for applications such as structural health monitoring and security surveillance in telecom, power grids, industrial manufacturing, and smart city infrastructure. However, conventional standard single-mode fibers (SSMF) are constrained by low intrinsic Rayleigh backscatter, which limits sensing range and sensitivity. To address this challenge, we developed Enhanced Scattering Fiber (ESF), known commercially as DataSens™ (DS) fiber, to provide higher optical backscatter and better acoustic sensitivity.

This paper presents results from a comprehensive set of field trials evaluating the DAS performance of ESF-based DS cables deployed in diverse environments, including conduit-buried and aerial installations, and within both linear and Passive Optical Network (PON) configurations. Controlled vibration events—such as weight drops, human footsteps, and drone flyovers—were introduced to represent realistic operational scenarios. Three major results were obtained. First, DS cables delivered substantially stronger DAS responses than SSMF, particularly in long-reach, photon-limited conditions, enabling enhanced detection of weak or distant vibration events and extending overall sensing coverage. Second, DAS operation beyond PON splitters was experimentally verified, with DS cables and fiber delay lines enabling clear identification of vibration events along individual distribution fibers. This result confirms the feasibility of DS cable for shared sensing- telecom network applications. Third, eleven cable configurations using AllWave® (AW) and DS fibers were evaluated over short-reach (~10 km) and long-reach (>50 km) scenarios. The field results provide practical guidance for optimizing fiber type and cable design to improve DAS performance in both dedicated and integrated network deployments.

Keywords: Distributed acoustic sensing, Enhanced Scattering Fiber, Passive Optical Network, structural health monitoring, Security surveillance

1. INTRODUCTION

Distributed Acoustic Sensing (DAS) has emerged as a transformative solution for real-time, large-scale vibration monitoring in applications such as pipeline surveillance, perimeter security, transportation infrastructure and smart city. However, DAS performance has traditionally been limited by conventional single-mode fiber based on Rayleigh backscatter, and standard cable designs. Lightera has recently introduced DataSens™, an advanced optical fiber specifically engineered for DAS applications. Enabled by ESF, DS delivers more than 10 times the scattering signal compared to single-mode fiber (SMF), significantly boosting the performance of DAS systems. Importantly, this increase in backscatter is achieved without degrading key optical properties: attenuation levels and splicing behavior, and overall fiber compatibility remain comparable to conventional standard SMF. As a result, DataSens™ fibers offers a practical upgrade for telecom-style deployments while providing significant performance gains for sensing applications.

To demonstrate the capabilities and understand the properties of this new fiber, Lightera fabricated two different test cables, each incorporating a mix of DS and standard AllWave® (AW, G.652/G.657A1) fibers. The first cable was a Lightera Fortex® DT model, designed with dedicated subunits for sensing and communications, and manufactured at Carrollton, GA facility. The second cable was a Specialty cable produced at the Avon, CT site, featuring a smaller fiber count but optimized for enhanced DAS performance through tighter mechanical coupling and higher sensitivity. These cables were installed in a testbed behind the Carrollton plant, spanning both conduit-buried and aerial segments to simulate various real-world installation conditions.

In collaboration with Sintela and FiberSense, Lightera conducted a comprehensive series of DAS field trials across both linear and PON configurations to assess the response of the fibers to a range of acoustic stimuli. This paper presents a summary of the field trial results which highlight how DS fiber enables high sensitivity, long sensing range operation, and seamless integration into telecom-style cable designs, positioning it as a breakthrough solution for next-generation sensing infrastructure

2. FIELD TRIAL SETUP

Figure 1 (a) and (b) illustrate the structural configurations of the two test cables developed for the DAS field trial, emphasizing the different design consideration behind the Fortex® DT commercial cable and the Specialty Cable from Lightera’s Avon facility.

Fortex® DT is an established telecommunications grade cable, with a decades long legacy of being offered for commercial product as a GR-20 compliant outside plant cable. For this experiment a custom run of a 6-subunit Fortex DT cable was fabricated as a hybrid structure combining both standard telecom subunits and sensing-optimized subunits with DS and standard AW fibers. This cable will be referenced as “Fortex” in this paper, though it is a custom configuration and differs from the commercially available cable. Three types of subunit constructions were used, each distinguished by material composition and fiber content:

- a) Low Smoke Zero Halogen (LSZH) tight buffered Subunits– These subunits contained a single fiber per tube and were designed for improved sensing sensitivity by tight buffering and for fire safety. The fibers were color-coded and labeled as BL_BL: AW and OR_OR: DS fibers.
- b) Polybutylene Terephthalate (PBT) Gel-Filled Subunits– These subunits were filled with water blocking gel and housed two fibers per subunit. They were labeled: GR_OR: AW fiber, GR_BL: DS fiber
- c) Polypropylene (PP) Dry Loose Subunits – These subunits were a standard telecom tube design. Each subunit contained 12 fibers, which aligns with how this subunit is usually offered for commercial sale, as the loose structure allows easy access to individual fibers for connection and splicing operations.

This mix of materials and subunit configurations in the Fortex DT cable enabled integrated evaluation of sensing performance across different tube constructions and fiber densities—crucial for understanding tradeoffs between optimal cable design for sensing and established telecommunications design best practices.

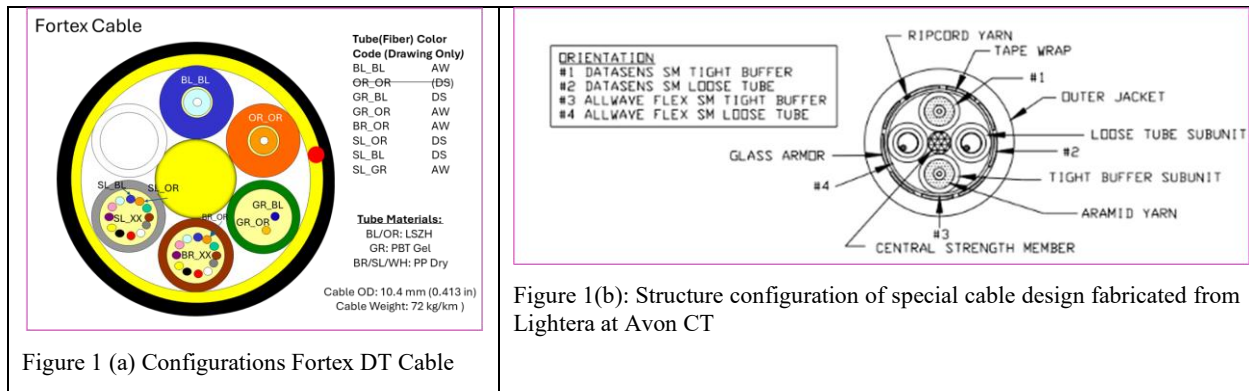


Figure 1 (a) Configurations Fortex DT Cable

Figure 1(b): Structure configuration of special cable design fabricated from Lightera at Avon CT

The Specialty Cable from Lightera’s Avon facility was a purpose-built sensing cable. It incorporated four fibers —two AW and two DS—using a combination of loose tube and tight-buffer constructions. This low fiber count design allowed for high mechanical coupling and good control over fiber placement, optimizing the structure for DAS sensitivity and clear signal contrast between the two fiber types. This cable platform lacks the structure needed for robust installation into conduit and aerial locations, though it was performed for this trial.

Together, these two cable designs provided a comprehensive platform for benchmarking the performance of DS versus standard fibers and different cable architectures and installations.

Figure 2 shows the layout of the testbed area situated directly behind Lightera’s Carrollton facility, where both cables were installed. The route map illustrates how the cables were deployed across a combination of underground conduits and aerial spans, closely replicating realistic installation conditions commonly encountered in telecommunications networks. This

mixed-installation environment enabled comprehensive evaluation of DAS signal performance under realistic deployment scenarios.

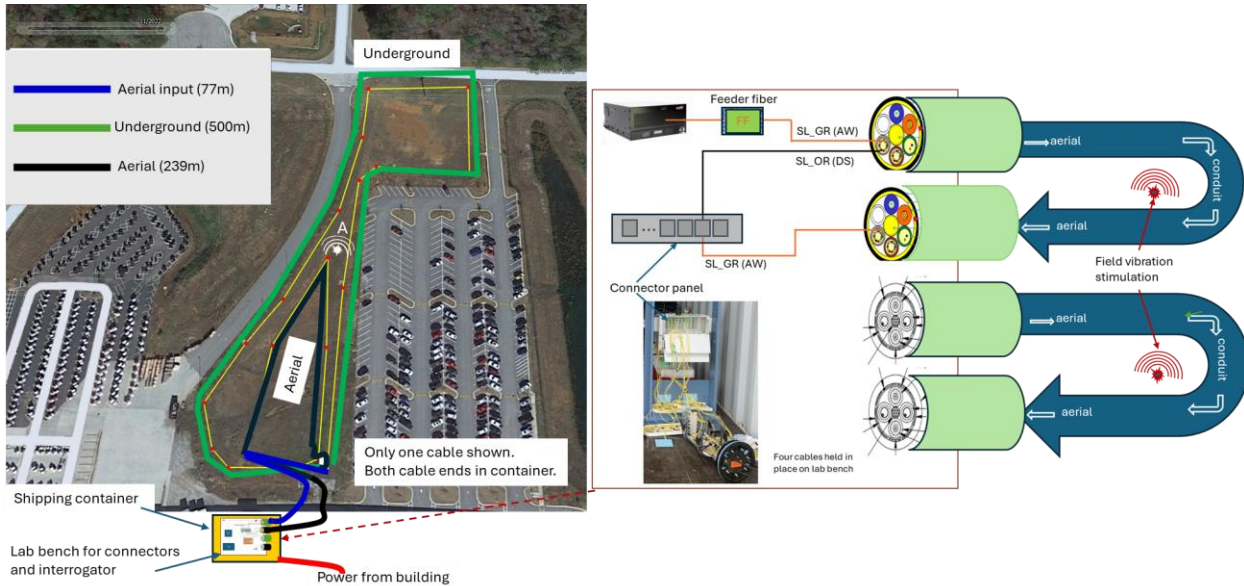


Figure 2, The field trial route, inset: DAS signal path for two fibers in the Fortex DT cable

As shown in Figure 2, the DAS signal path was deliberately configured to collect DAS signals from the same pathway through the cables, but in different fiber types. This allowed for a direct comparison of DAS performance at all times, since each cable type experienced the same acoustic signals. The side-by-side comparison could therefore be used with any type of acoustic signal, even the noisy signals appearing on aerial cable installations. The sequence was as follows: The interrogator launched the DAS signal into AW fiber within a 77m aerial span. The signal then passed through a 500-meter underground conduit segment, also using AW fiber. It continued into a 239m aerial AW fiber segment, completing the AW fiber portion with the signal travel distance to a total 816 m. The signal looped back to a connection panel, where it was then re-launched into the DS fiber that followed the same path: the DAS signal entered the 77-m DS fiber aerial section, followed by a 500m DS fiber underground conduit. Finally, it went to 239-m DS fiber aerial span, bringing the total two-loops signal travel distance to 1632 meters. Additional feeder fibers (FF) spools were added to each fiber at the beginning of the network to increase network length for various scenarios, which will be discussed later.

This hybrid routing configuration, alternating between AW and DS fibers across both aerial and buried installations, was carefully designed to allow direct performance comparisons between the two fiber types under identical physical and environmental conditions. By analyzing the DAS signal response from each segment, the testbed offers a robust platform for evaluating long-range sensitivity, signal integrity, and overall suitability for real-world DAS deployments using mixed cable architectures.

Following installation, WDM-OTDR measurements were performed on the DS fibers to characterize backscatter levels across the various cable segments. All DS fibers exhibited the expected wavelength-dependent scattering enhancement in the spectral regions relevant to DAS operation, except for the OR_OR subunit, whose enhanced-scattering band fell outside the operational wavelength of the interrogator. Consequently, the OR_OR subunit was excluded from the DAS field trials.

To evaluate real-world sensing performance, the installed fibers were connected to phase-based DAS interrogators from Sintela (the ONYX™ *peta* [1] and ONYX™ *peta-EX* models [2]). A series of controlled vibration events were conducted to probe the system's sensitivity and resolution. These acoustic stimuli included: Manual weight-drop strikes to simulate short, high-energy impulse events; Walking tests along the cable route to assess low-frequency, low-amplitude response; Drone overflights to evaluate airborne and coupling-limited signal detection.

3. FIELD TRAILS RESULTS AND DISCUSSION

3.1 Enhanced DAS Performance

Several experiments were conducted to evaluate the DAS performance of DS cables under a range of installation and excitation conditions. The first experiment focused on the Fortex® cable using the configuration shown in the inset of Figure 2, but without feeder-fiber (FF) spools to ensure that all test signals interacted directly with the installed field segments. In this setup, the DAS interrogator launched the sensing signal into the SL_GR AW fiber. At the connection panel, the signal was looped back into the SL_OR DS fiber, enabling a direct, same-path comparison between the two fiber types under identical environmental and mechanical conditions. To assess sensing performance comprehensively, the previously described simulated vibration events were introduced at various locations along both the buried and aerial cable sections.

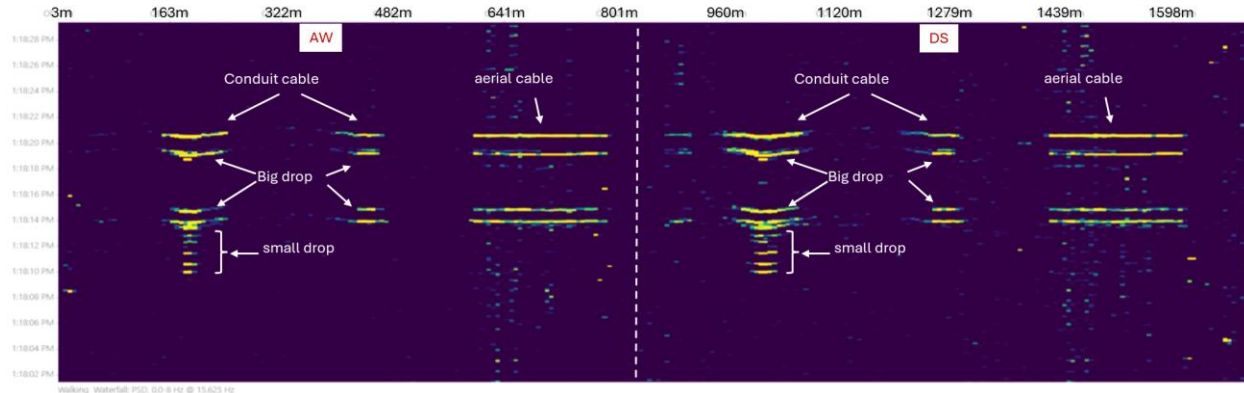


Figure 3, Waterfall charts for a sequence of vibration events including separate heavy drops followed by consecutive lighter drops

Figure 3 shows waterfall plots of the DAS response for a sequence of controlled weight-drop events conducted at the A point (shown in Figure 2), where both conduit and aerial cables exhibited measurable responses. The test sequence consisted of two large-mass drops using 15-lb weight followed by six consecutive smaller-mass drops using a 2-lb weight. The results reveal several important trends: The 15-lb drops generated strong, high response of DAS signals that were clearly detected in both the conduit and aerial cable segments. The 2-lb drops produced weaker vibrations that were detectable only in the conduit-buried segment closest to the impact location. Both AW and DS fibers successfully detected vibration events; however, the DS fiber consistently produced higher-intensity DAS responses, while the AW fiber exhibited lower signal response. These findings confirm that, while both fiber types are capable of sensing a broad range of vibration events, DS fibers cable deliver a clear sensitivity advantage in DAS applications, particularly for detecting low-amplitude or marginally coupled disturbances.

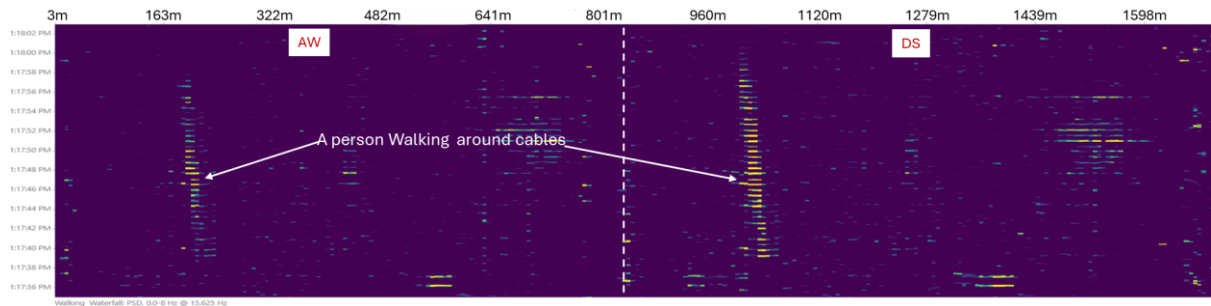


Fig. 4 Waterfall charts for a person walking around field around cables

Fig. 4 displays the DAS signals captured as a person walks in the field at the location of the buried sensor cable area. Both AW and DS cable design work well, as the individual approaches, the DAS response increases in intensity, reflecting the growing proximity of the vibration source. Notably, the stronger signal observed on the right side of the figure corresponds to the DS cable. This indicates that the DS cable exhibits higher sensitivity to the footstep-induced ground vibrations compared to the AW cable. The clear contrast in signal amplitude highlights the enhanced acoustic coupling and

responsiveness of the DataSens design, making it more effective for detecting subtle or distant vibration events in buried applications.

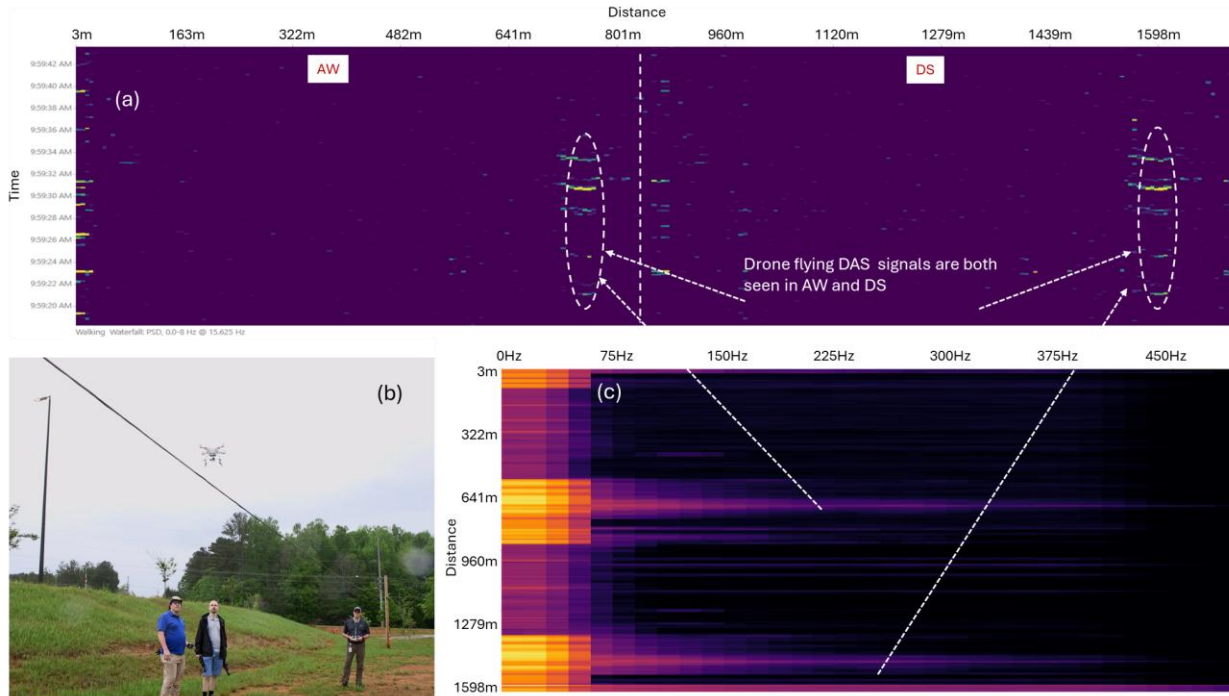


Fig. 5 (a) Waterfall charts for when a small drone flew over the aerial cables (b), (c) the two-dimensional PSD distribution as a function of both frequency and distance.

Figure 5(a) displays waterfall plots of the DAS signals recorded by the Peta interrogator during a drone-overflight test above the aerial cable installation shown in Figure 5(b). The DJI Phantom 3 Standard drone (approximately 3 lb, with 3 m/s ascent and 5 m/s descent capabilities) generated airborne acoustic and mechanical vibrations that were successfully detected by both AW and DS (PP-dry) cables. A subsequent power-spectral-density (PSD) analysis, shown in Figure 5(c), reveals the spatial and spectral characteristics of the event as a function of distance and frequency. The DS fiber response—shown on the right side of each plot—was slightly stronger than that of the AW fiber, suggesting improved sensitivity to high-frequency, low-amplitude vibrations associated with drone rotors. These results demonstrate that both cable types can detect airborne disturbances, with DS offering a performance margin under weak-coupling conditions.

The second experiment incorporated a 30-km FF as illustrated in Figure 2. Here, the DAS signal was first launched into a 30-km AW fiber spool housed in a vibration-isolated enclosure to ensure the feeder contributed no external noise. After propagating through the feeder fiber, the signal entered an AW sensing segment, looped back at the connection panel, and was then directed into the DS fiber for the return path.

To evaluate and compare sensing-sensitivity under long-reach, photon-limited conditions, controlled vibration events were again introduced. Figures 6(a) and 6(b) show waterfall plots for two cable designs tested: (1) Specialty-Cable (#4 AW and #2 DS, loose-tube), and (2) Fortex® PBT gel-filled cable (AW: GR_OR, DS: GR_BL). In both cases, three 15-lb weight drops were performed from identical heights and at the same physical location. For both cable designs, the AW fiber segments produced little to no detectable DAS signal due to significant attenuation accumulated over the 30-km feeder—resulting in a “photon-poor region” with insufficient backscatter to support acoustic sensing.

In contrast, the DS fibers—despite being positioned after the same lossy feeder and operating at even lower optical power—successfully detected all three vibration events with clear signatures. This demonstrates the superior acoustic sensitivity and backscatter efficiency of the DS design, particularly in long-reach or power-limited scenarios. The ability of DS fiber to register meaningful signals under such challenging conditions underscores its suitability for buried, remote, and extended-reach DAS deployments where reliable detection of weak or distant events is critical.

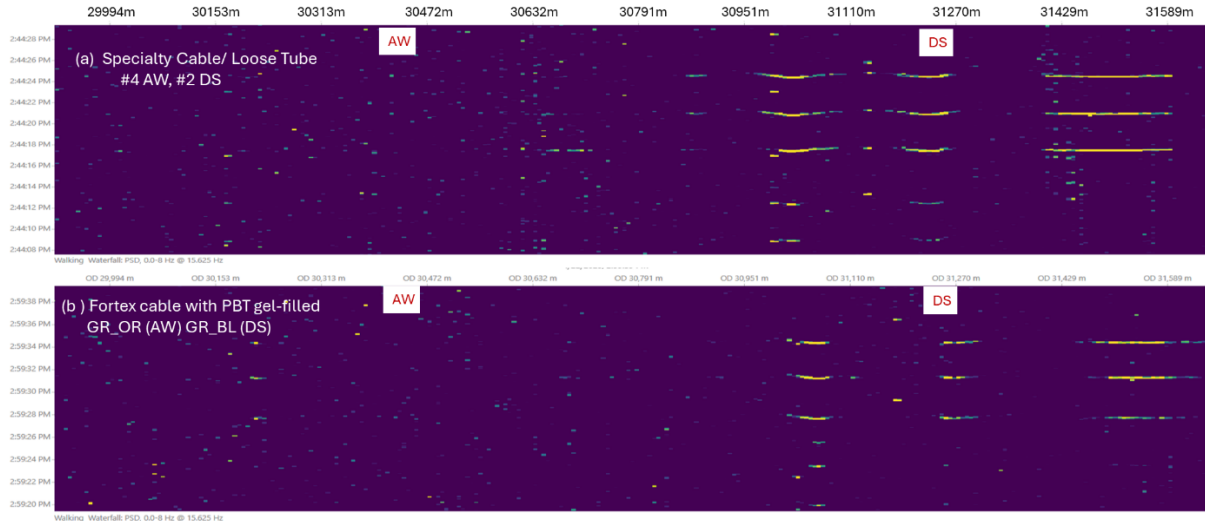


Fig. 6: Waterfall plots corresponding to the three cable designs tested: (a) specialty cable/ loose-tube cable, and (b) Fortex PBT gel-filled constructions.

3.2 DAS over Passive Optical Network Schemes

DAS over Passive Optical Network (PON) architecture has emerged as a promising research direction with potential applications across a wide range of sectors. These include broadband access networks, next-generation wireless infrastructure such as 5G and future 6G, smart power grids, and industrial monitoring for manufacturing environments [3]. However, several technical challenges must be addressed to realize practical and robust DAS implementations over such architectures. First, DAS operates by launching optical pulses into the fiber and analyzing the returning Rayleigh backscattered light to infer dynamic strain variations along the fiber length. Unlike conventional data transmission, DAS depends on the round-trip measurement of the backscattered signal. As a result, signal attenuation is effectively doubled in dB, making DAS systems particularly sensitive to propagation losses. This limitation becomes more pronounced in PON environments where passive optical splitters introduce significant loss, and the distribution fibers (DFs) between the splitter and the optical network units (ONUs) are often relatively short. These factors collectively reduce the already weak Rayleigh backscatter signal to levels that may fall below the detection threshold of standard DAS interrogators. To overcome this limitation, we have recently proposed and experimentally validated a novel DAS-over-PON scheme that utilizes ESF in the DF segment [3]. ESF significantly increases the backscatter level, thereby improving DAS signal strength even in high-loss, splitter-based configurations. Here, we summarize the field trial evaluations to assess the sensing performance of DAS over PON.

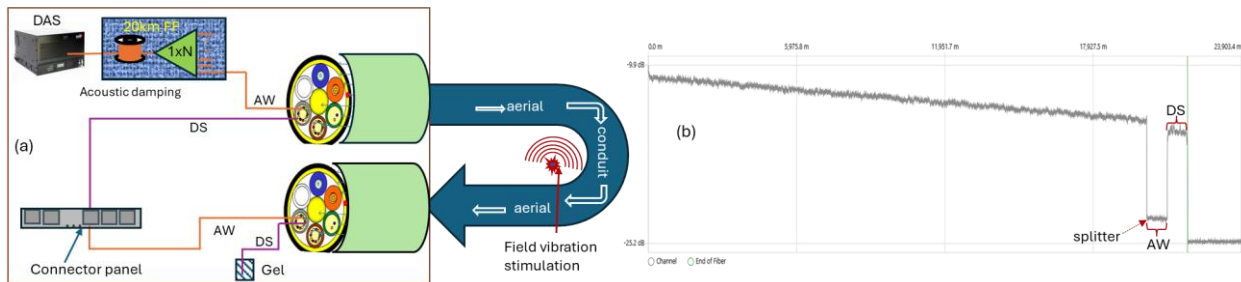


Fig. 7 (a): Schematic diagram of the experimental setup for DAS over PON scheme, (b) the OTDR trace from 1x8 splitter measurement.

Fig. 7 (a) shows the schematic diagram of the experimental setup designed to evaluate DAS operation over a PON configuration. In this setup, the optical sensing signal generated by the interrogator was first launched into a 20 km FF before entering a $1 \times N$ optical fiber splitter. To minimize unwanted interference, both the feeder fiber spool and the splitter were placed inside a vibration- and acoustically isolated box. From the splitter, one output port was connected to AW fiber of the installed test cable, and the DAS signal traveled along the test cable path, which consisted of an aerial cable section, followed by an underground conduit segment, and then another aerial cable section. At the connector panel, the signal was

looped back and routed into the DS fiber of the same cable, and it went the same physical route as AW fiber path. To prevent Fresnel reflections and associated signal artifacts at the terminal end, the end of DS fiber was immersed in index-matching gel.

Fig. 7 (b) plots the OTDR trace obtained from a measurement for a 1x8 splitter using a Peta interrogator. The trace shows a significant drop in signal amplitude at the location of the splitter, following the initial 20 km propagation through the FF. This decrease is primarily due to the intrinsic insertion loss of the splitter, combined with the signal reduction already incurred over the FF span. After entering the AW fiber, the OTDR signal maintained low. However, the OTDR signal increased significantly when it passed through the DS fiber, which was constructed using DS fiber with ESF. The high scattering level in ESF substantially improves the DAS signal-to-noise ratio, particularly in the high-loss configurations such as those involving passive optical splitters. The practical impact of this difference is illustrated in Fig. 8, which presents a recorded waterfall chart from a controlled field test using Peta interrogator. In this test a 2 lb weight was dropped to induce a localized vibration event. The vibration was clearly detected along the DS fiber path, appearing as a distinct and time-localized feature in the DAS output. In contrast, no measurable sensing signal was observed along the AW fiber path under identical conditions. This absence of detection confirms that, after the combined losses from the FF and the splitter, the already low Rayleigh backscatter of the AllWave fiber falls below the DAS detection threshold. These results highlight the critical role of ESF with high scattering characteristics in enabling real DAS applications over PON architecture.

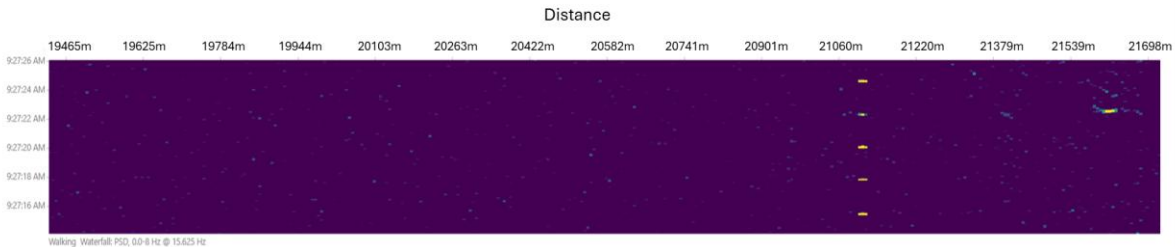


Fig. 8: recorded waterfall chart for 1x8 splitter PON from a controlled field test using Peta interrogator with a 2 lb weight drops

A second challenge in implementing DAS over PON architecture is the difficulty to distinguish sensing signals originating from individual DFs and their corresponding ONUs. In PON configurations, the backscattered signals from each DF segment are superimposed, thus complicating the task of isolating and interpreting sensing data from specific remote fiber branches. To address this issue, we have recently proposed and experimentally demonstrated a solution that combines ESF with intentionally introduced fiber delays in the DF segment [3]. By inserting fiber spools of varying lengths—acting as optical delay lines—in the remote node, each DF/ONU path is assigned a unique time offset. This approach temporally separates the backscattered responses from different branches, enabling the DAS system to distinguish between signals from multiple reflection paths. Here, we summarize the results of the field tests conducted to demonstrate the effectiveness of this ESF with delay scheme in resolving multiple sensing paths within a PON configuration.

Fig. 9 illustrates the schematic diagram of the experimental setup, which utilized Avon’s Specialty-cables. In this configuration, the optical sensing signal generated by the DAS Peta interrogator was directly connected to a 1×N (N=16) optical fiber splitter. Two output ports from the splitter were used to create parallel sensing paths, enabling sensing measurement with delay-based signal separation. The first output port, which is designated channel 1, was connected to the AW fiber (#4) of the installed Specialty-cable. The DAS signal propagated along the same composite cable route, comprising an aerial span, followed by an underground conduit section, and then another aerial span. Upon reaching the connector panel, the DAS signal was looped back and returned through the DS fiber (#2) in the same cable, propagating the identical physical path. The second output port of the splitter, which is called channel 2, was routed through a 2-km SCUBA125 fiber spool, which served as an optical delay line. The SCUBA125 fiber has ultra-large effective area (A_{eff}) of $125\mu m^2$ and ultra-low attenuation [4], and lower Rayleigh scattering than Ge-doped standard SMF, which generates less DAS response than standard SMF. This delayed signal was then injected into the AW fiber (#3) of the Specialty-cable. As with the first path, the signal followed the aerial–conduit–aerial cable route and was looped back via the corresponding DS fiber (#1), again traveling along the same physical infrastructure. The intentional delay introduced in the second path enabled spatial separation of the backscattered signals from each branch during DAS signal processing.

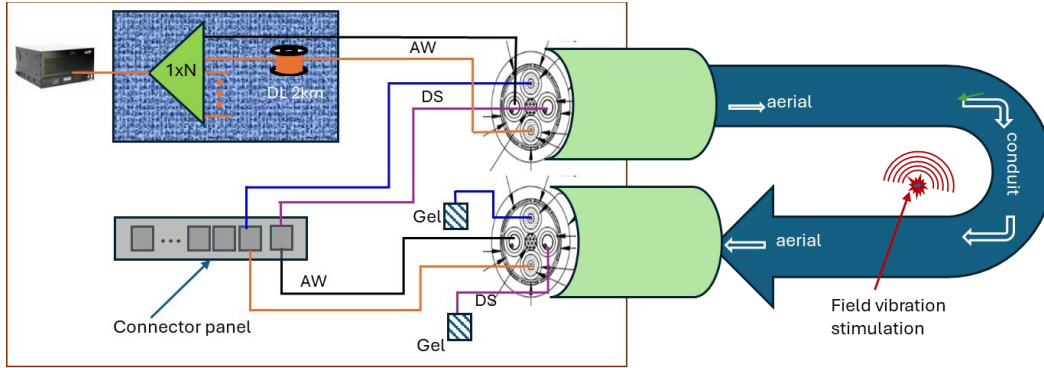


Fig. 9 Schematic diagram of the experimental setup for DAS over PON scheme with the delayed fiber line

Fig. 10 presents a recorded DAS waterfall chart from the field test conducted using the Peta interrogator. In this experiment, a 2lb weight was dropped to generate a localized vibration event along the cable route. The vibration signals from Channel 1, corresponding to the DS fiber path through the Specialty-cable #2, were clearly detected. Moreover, the two sensing channels—originating from Port 1 and Port 2 of the optical splitter—through DS fiber in Specialty-cable #2 and Specialty-cable #1 were successfully distinguished as separate traces in the DAS output. It is important to note that no measurable sensing signals were detected along the AW fiber paths through the specialty cable #4 and specialty cable #3 on either channel. This absence is attributed to the combination of using the Peta interrogator—a lower-performance version of the interrogator—and a 1×16 passive optical splitter, which together introduced significant loss and reduced the backscatter level of the AW fiber below the DAS detection threshold.

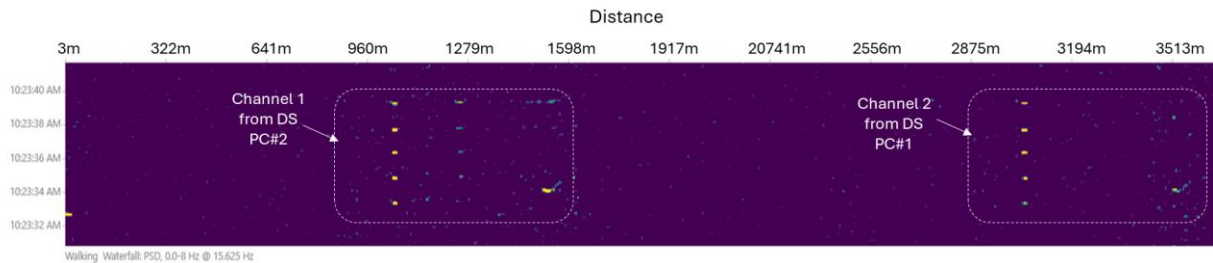


Fig. 10 Recorded DAS waterfall chart showing the two sensing channels from Port 1 and Port 2 through DS fiber in specialty cable #2 and specialty cable #1 (from Avon’s specialty cable) were successfully distinguished

3.3 DataSens Fiber Cable Design Comparison

Three sequential field experiments were conducted to evaluate the DAS performance of a set of eleven fiber cables incorporating two cable types: Avon’s Specialty-cable and Carrollton’s Fortex® DT cable using AW and DS fibers. The cables were connected in series (configuration S1), as summarized in Table 1.

The experimental configuration for the first test is illustrated in Fig. 11(a). The optical sensing pulses generated by the Peta interrogator were launched with 12 dB attenuation to ensure optimal DAS operation by mitigating nonlinear effects while maintaining adequate SNR. The signal first propagated through a 10 km SMF FF housed in a vibration- and acoustically isolated enclosure. Upon exiting the FF, the signal entered the first AW fiber (BL_BL) of the installed cable route, traversing an aerial span, an underground conduit, and a second aerial span. At the connector panel, the signal was looped back into the next AW fiber (BR_OR), propagating along the same aerial–conduit–aerial path. This loopback sequence continued through the full set of eleven cables, comprising six AW fibers followed by five DS fibers.

Figure 11(b) shows the OTDR trace measured using the Peta interrogator. A slight signal drop was noticed at connection points along the first six AW fibers. In contrast, for the DS fiber segments (cables 7–11), the reflected signal amplitude was increased significantly, attributed to the enhanced backscattering provided by ESF. Notably, DS fibers in the 9th (Specialty-cable #2) and 11th (Specialty-cable #1) cable exhibited slightly higher enhancement compared to other DS fibers.

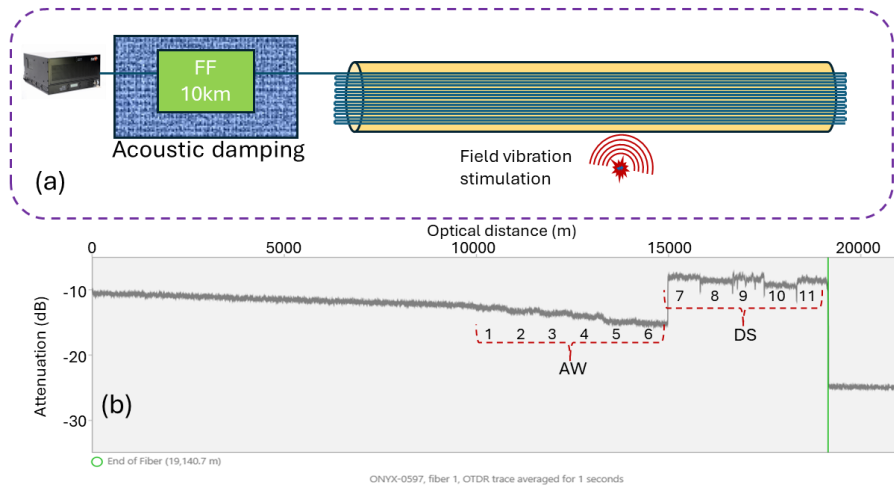


Table 1: serial order of testing fibers

Name	Serial order	Tube type	Fiber
BL_BL	1	LSZH	AW
BR_OR	2	PP Dry	AW
SL_GR	3	PP Dry	AW
Specialty cable #4	4	Loose tube	AW
GR_OR	5	PBT Gel	AW
Specialty cable #3	6	Tight Buffer	AW
SL_OR	7	PP Dry	DS
SL_BL	8	PP Dry	DS
Specialty cable #2	9	Loose Tube	DS
GR_BL	10	PBT Gel	DS
Specialty cable #1	11	Tight buffer	DS

Fig.11 (a) A schematic of the experimental setup, (b) measured OTDR trace with 10km FF using the Peta interrogator

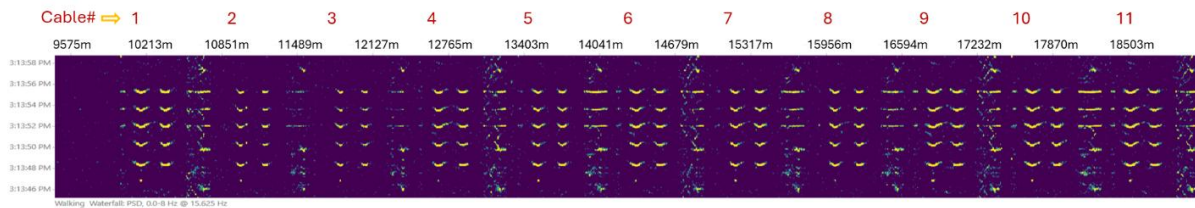


Fig. 12 Recorded DAS waterfall chart from the field tests with five 15-lb weight drops to generate distinct vibration events

Figure 12 presents the DAS waterfall chart for five 15-lb weight-drop events applied at Point A of Fig. 2. All eleven cables successfully detected vibration events across the near and far conduit sections as well as the aerial segment. Cables 9, 11, 1, and 10 produced the strongest responses, whereas cables 2 and 3 exhibited weaker responses.

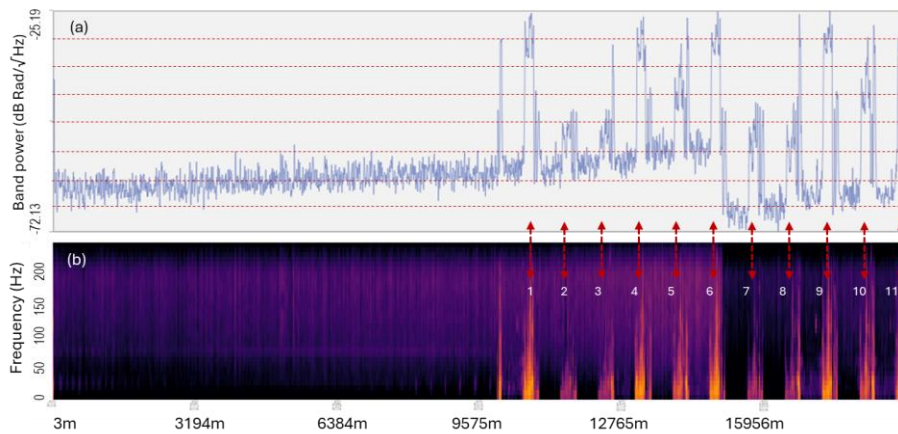


Table 2: cables' serial order & SNR

Cable Name	Serial order	Tube type	Fiber	SNR (dB)
BL_BL	1	LSZH	AW	32.2
BR_OR	2	PP Dry	AW	9.5
SL_GR	3	PP Dry	AW	12.0
Specialty cable #4	4	Loose tube	AW	29.5
GR_OR	5	PBT Gel	AW	22.9
Specialty cable #3	6	Tight Buffer	AW	28.5
SL_OR	7	PP Dry	DS	21.9
SL_BL	8	PP Dry	DS	25.3
Specialty cable #2	9	Loose Tube	DS	36.8
GR_BL	10	PBT Gel	DS	30.7
Specialty cable #1	11	Tight buffer	DS	35.6

Fig. 13 (a) PSD in dB rad/√Hz versus sensing distance from spectrum analysis, (b) 2-D (frequency -distance) PSD data in 10km FF experiment.

To evaluate the performance of each cable design, we performed a power spectral density (PSD) analysis over 0–150 Hz frequency range, then estimated the acoustic signal-to-noise ratio (SNR). An example of the PSD analysis is shown in Fig. 13(a), which plots the PSD in dB rad/√Hz versus sensing distance. Interestingly, the noise levels from FF and AW of the installed fiber cables increases linearly in dB (Rad/Hz) plot, the DS fiber suppresses the noise level more than 10dB. The corresponding two-dimensional PSD distribution, shown in Fig. 13(b), maps PSD values as a function of both frequency and distance, revealing the spatial and spectral characteristics of the sensing response. Because all fibers share the same

physical route, the relative amplitudes of these aerial-segment responses provide a direct measure of each cable’s intrinsic acoustic sensitivity. Conversely, low-signal regions—such as FF and conduit spans—primarily reflect the noise floor of the DAS system.

As shown in Fig. 13(a), cable #1 (LSZH tight buffer) produced the strongest response among the AW fibers, while #2 and #3 (PP-dry) performed poorest. All five DS fibers exhibited significantly lower noise floors and higher backscatter, with Specialty-cable #2 (cable 9, loose-tube) and Specialty-cable #1 (cable 11, tight-buffer) outperforming the PP-dry DS designs. SNR values, estimated from PSD data and averaged over three measurements, are reported in Table 2.

The second experiment used the same setup as Fig. 11(a), except that the 10 km FF was replaced by 50 km of SMF. A 9 dB attenuation was applied at the interrogator output to maintain optimal DAS operation. The cable order remained identical to previous one. Figure 14(a) shows the OTDR trace. A slight change in slope is visible when transitioning from the 50 km FF into the installed AW cables, indicating marginally higher attenuation in the latter. A significant increase in backscattered power appears in the DS cable sections (cables 7–11), again due to the high scattering gain provided by the ESF. Specialty-cable #2 (cable 9) and Specialty-cable #1 (cable 11) exhibited the strongest backscatter enhancement.

Figure 14(b) shows the corresponding DAS waterfall chart. Among the six AW cables, only cable #1 (LSZH) detected vibration through the near-conduit region, and even then with weak amplitude. In contrast, all five DS cables produced clear vibration signatures after 50 km of transmission. Cables 9 and 11 delivered the strongest DS-fiber responses, while cables 7 and 8 produced weaker but still detectable signals.

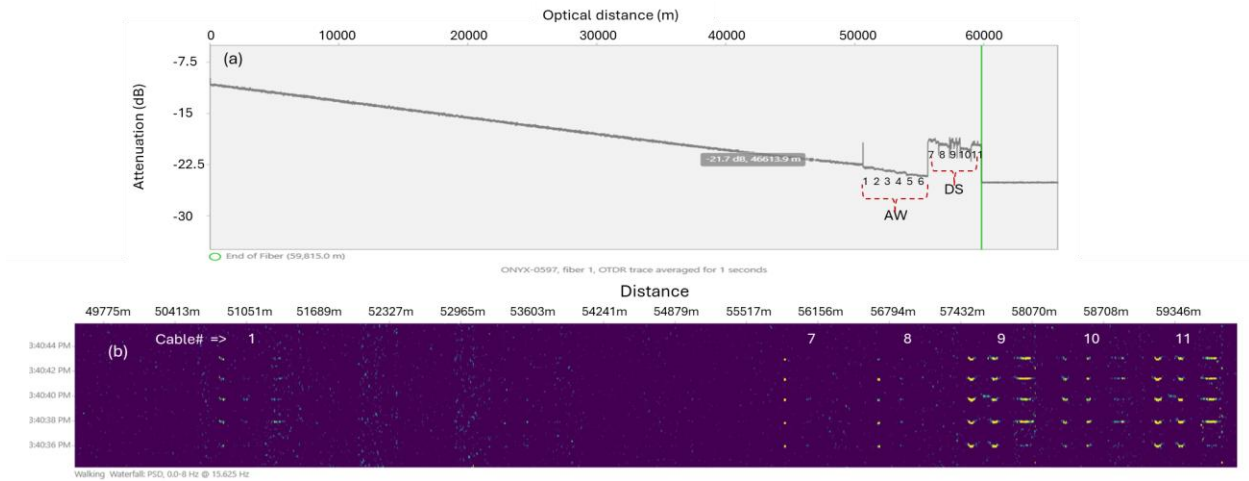


Fig. 14 (a) measured OTDR trace with 50km FF, (b) Recorded DAS waterfall chart with five 15-lb weight drops.

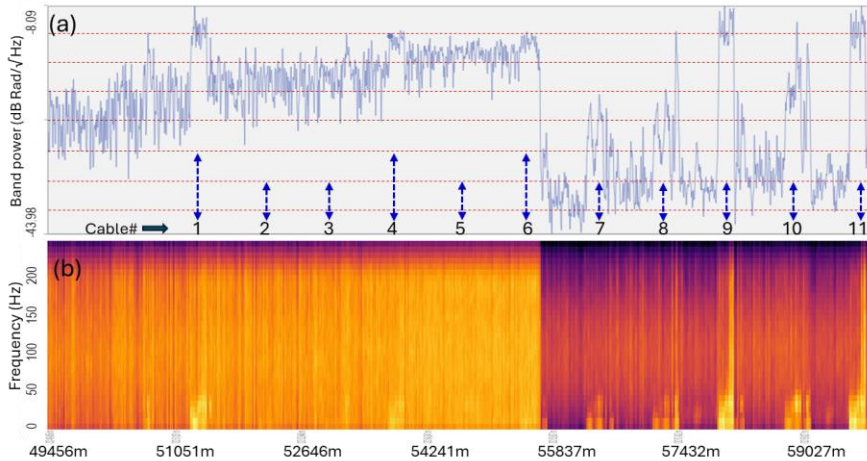


Table 3: cables’ serial order & SNR (50km FF)

Name	Serial order	Tube type	Fiber	SNR (dB)
BL_BL	1	LSZH	AW	8.1
BR_OR	2	PP Dry	AW	0.0
SL_GR	3	PP Dry	AW	0.0
Specialty cable #4	4	Loose tube	AW	2.5
GR_OR	5	PBT Gel	AW	0.0
Specialty cable #3	6	Tight Buffer	AW	1.1
SL_OR	7	PP Dry	DS	9.5
SL_BL	8	PP Dry	DS	10.2
Specialty cable #2	9	Loose Tube	DS	23.6
GR_BL	10	PBT Gel	DS	12.3
Specialty cable #1	11	Tight buffer	DS	21.7

Fig. 15 (a) PSD in dB rad/√Hz versus sensing distance from spectrum analysis for 50km FF experiment, (b) PSD values as a function of both frequency and distance (ie. spatial and spectral characteristics of the sensing response)

PSD analysis (0–150 Hz) was again performed. Example spectra and 2D PSD maps are shown in Fig. 15(a) and Fig. 15(b). Three AW fibers produced marginal signals: cable #1 (LSZH), cable #4 (Specialty-cable #4), and cable #6 (Specialty-cable #3). The remaining AW fibers—two PP-dry and one PBT-gel—yielded no detectable responses. All DS fibers produced signals above the noise floor, with cables 9 and 11 again showing the highest sensitivity. SNR results averaged over three measurements are summarized in Table 3.

In the third experiment, the series order of the eleven cables was reversed (Fig. 11(a)) while maintaining a 50 km FF. A 9 dB attenuation was used to ensure stable DAS operation. Figure 16(a) shows the OTDR trace, confirming the expected enhancement in backscatter for all DS fiber segments. The corresponding waterfall chart in Fig. 16(b) shows that all DS cables detected the five 15-lb weight-drop events. Specialty-cable #1 (cable 11) and Specialty-cable #2 (cable 9) again exhibited the strongest responses, while cables 7 and 8 produced weaker signals. In contrast, none of the six AW cables produced measurable responses in this reversed-order configuration. Even cable #1 (LSZH), which showed marginal detectability in Experiment 2, fell below the DAS detection threshold. This outcome is consistent with the extremely low photon flux reaching the final fiber positions in deep photon-poor operation. PSD analysis (Fig. 17(a), (b)) was again performed, and SNR values averaged over three measurements are summarized in Table 4.

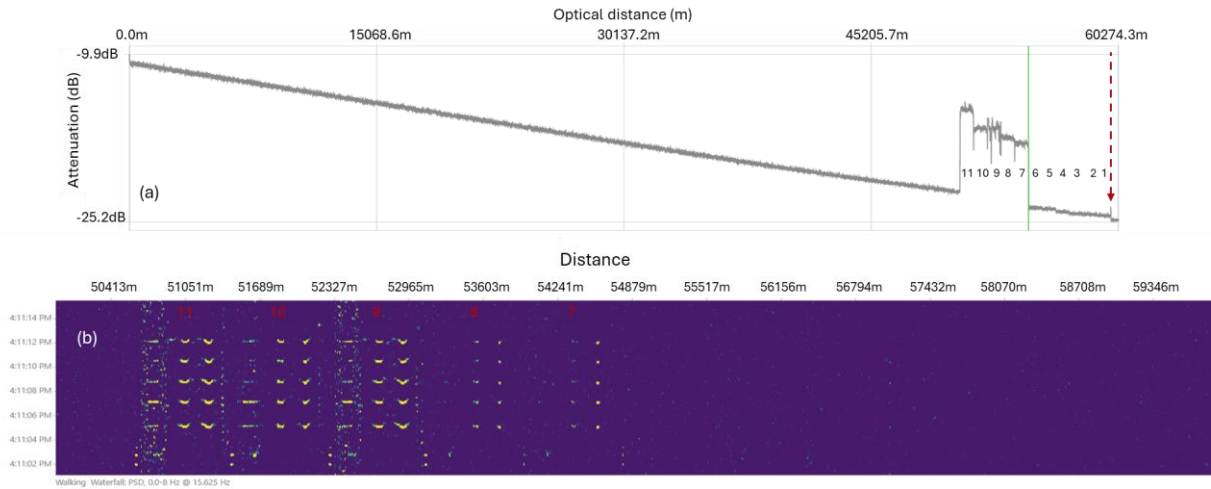


Fig. 16 (a) measured OTDR trace from 3rd experiment with reversed order of serail cable and 50km FF, (b) Recorded DAS waterfall chart with five 15-lb weight drops.

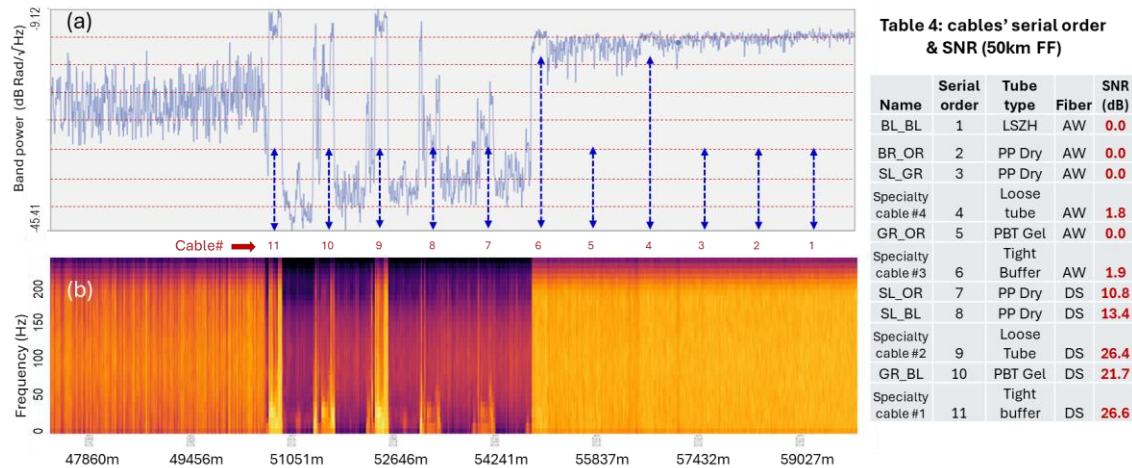


Fig. 17 (a) PSD in dB rad/√Hz versus sensing distance from spectrum analysis for 50km FF reversed-order experiment, (b) PSD values as a function of both frequency and distance

Across all three field trial experiments, a consistent trend emerged: within the short-reach (~10 km, photon-rich) region, the LSZH tight-buffered subunit (cable #1) performed competitively among AW-fiber designs. However, for longer-reach (>50 km, photon-poor) regime, the DS-fiber cables incorporating ESF consistently outperformed AW-fiber cables due to

their substantially enhanced Rayleigh backscatter. Across all 3 field trial experiments, a consistent trend emerged - within the short-reach (~10 km, photon-rich) region, AW fibers performed adequately. As distance increased, especially out to 50 km, the DS-fiber cables incorporating ESF consistently outperformed AW-fibers due to their substantially enhanced Rayleigh backscatter. Cable construction performance trends were also clear. As expected, tight-buffered designs generally exhibited superior acoustic sensitivity relative to loose-tube designs, and gel-filled designs outperformed totally dry designs. However, Avon’s loose-tube Specialty-cable #2 and Specialty-cable #4 performed comparably to their tight-buffered counterparts (Specialty-cable #1 and Specialty-cable #3). This behavior is likely attributable to the special loose-tube construction in which elevated mechanical pre-tension improves strain transfer and vibration coupling.

Table 5 SNR values from three field experiments

Name	Serial order (S1)	Tube type	Fiber	10km FF S1, SNR (dB)	50km FF S1 SNR(dB)	50km FF Reversed S1 SNR(dB)	50km FF Avg SNR(dB)
BL_BL	1	LSZH	AW	32.2	8.1	0.0	4.1
BR_OR	2	PP Dry	AW	9.5	0.0	0.0	0.0
SL_GR	3	PP Dry	AW	12.0	0.0	0.0	0.0
Specialty cable #4	4	Loose tube	AW	29.5	2.5	1.8	2.2
GR_OR	5	PBT Gel	AW	22.9	0.0	0.0	0.0
Specialty cable #3	6	Tight Buffer	AW	28.5	1.1	1.9	1.5
SL_OR	7	PP Dry	DS	21.9	9.5	10.8	10.1
SL_BL	8	PP Dry	DS	25.3	10.2	13.4	11.8
Specialty cable #2	9	Loose Tube	DS	36.8	23.6	26.4	25.0
GR_BL	10	PBT Gel	DS	30.7	12.3	21.7	17.0
Specialty cable #1	11	Tight Buffer	DS	35.6	21.7	26.6	24.2

4. CONCLUSIONS

The field trials presented in this study demonstrate that substantial gains in DAS performance can be achieved through informed selection of fiber type and cable construction. Across all experiments, DS fiber incorporating ESF technology consistently delivered higher acoustic sensitivity than conventional AW fiber, with the most pronounced improvements observed in long-reach and high-loss scenarios, including PON-based networks. The successful demonstration of DAS operation within a PON architecture further confirms that vibration events occurring along individual splitter branches can be reliably detected and distinguished using DS fiber and delay-line interrogation methods. This capability highlights the viability of cost-effective, dual-use communication-and-sensing deployments within existing access-network infrastructures.

Comparative evaluation of eleven cable designs revealed that both fiber construction and operational conditions exert significant influence on sensing performance. Within the Fortex® DT family, the tight-buffered subunit LSZH one-fiber design achieved an acoustic SNR advantage of approximately 10–20 dB relative to conventional telecom subunit designs under short-reach (~10 km) conditions. While tight-buffered cables generally provided the highest acoustic sensitivity, loose-tube designs from Avon’s Specialty-Cable series matched the performance of their tight-buffered counterparts. This behavior is likely attributable to specialized mechanical features that improved strain transfer to the fiber.

Collectively, these results offer clear, practical guidance for optimizing DAS system deployment. By appropriately pairing fiber type, cable construction, and network topology, operators can achieve high-sensitivity, robust distributed acoustic sensing across both dedicated and shared-network environments. These findings provide a framework for advancing large-scale, real-world DAS implementations and for accelerating the integration of sensing capabilities into modern fiber-optic communication infrastructures.

5. Reference

[1] <https://sintela.com/onyx-peta/>
 [2] <https://sintela.com/onyx-peta-ex/>
 [3] Benyuan Zhu, Yaowen Li, Paul S. Westbrook, Zhou Shi, Kenneth S. Feder, Ting Wang, and David J. DiGiovanni, "Distributed Acoustic Sensing Over PON Architecture by Using Enhanced Scattering Fiber," J. Lightwave Technol. 43, 6285-6290 (2025)
 [4] <https://fiber-optic-catalog.ofsoptics.com/documents/pdf/TeraWave-SCUBA-125-Single-Mode-fiber-170-web.pdf>